Density Functional Theory Investigation of the Binding of ThioTEPA to Purine Bases

Cherni, Emna; Adjieufack, Abel Idrice; Champagne, Benoît; Abderrabba, Manef; Ayadi, Sameh; Liégeois, Vincent

Published in:
Journal of physical chemistry A

DOI:
10.1021/acs.jpca.0c01792

Publication date:
2020

Document Version
Publisher's PDF, also known as Version of record

THE JOURNAL OF PHYSICAL CHEMISTRY A

pubs.acs.org/JPCA Article

Density Functional Theory Investigation of the Binding of ThioTEPA to Purine Bases: Thermodynamics and Bond Evolution Theory Analysis

Published as part of The Journal of Physical Chemistry virtual special issue "Paul Geerlings Festschrift".

Emna Cherni, Abel Idrice Adjieufack, Benoît Champagne,* Manef Abderrabba, Sameh Ayadi, and Vincent Liégeois*

Cite This: *J. Phys. Chem. A* 2020, 124, 4068–4080 Read Online

ABSTRACT: Density functional theory with the ωB97X-D exchange–correlation functional together with implicit as well as explicit solvation is used to describe the reactions of the adenine and guanine purine bases on *N*,*N*′,*N*″-triethylenethiophosphoramide (thioTEPA), an alkylating agent used as an anticancer drug. This reaction is decomposed into (i) a nucleophilic addition and (ii) a proton "migration" that is mediated by the solvent molecules. The calculations reveal that the first step is rate determining and that the presence of an explicit water molecule to mediate the proton migration has a negligible role on the kinetics of the first step, so that the focus is set on the first step of the reaction. ωB97X-D calculations highlight (i) the activation energy (Gibbs free enthalpy) is smaller for imine nitrogens than amine nitrogens, (ii) for the imine functions, the activation energy is slightly smaller for adenine than for guanine together with a larger exergonicity for the alkylation by adenine, and (iii) among the amine nitrogens, the presence of stabilizing H-bonds in the case of exocyclic amines leads to smaller activation energy than for the endocyclic ones. The reaction mechanisms are unraveled by employing the bond evolution theory, combining the use of electronic localization functions, and their evolution along the intrinsic reaction coordinate, with Thom's catastrophe theory. These analyses, suitable for highlighting the populations of the major monosynaptic and disynaptic basins, show (i) the reaction with imine nitrogens begins by the cleavage of the C–N aziridine bond and is followed by the simultaneous formation of the new C–N bond and the disappearance of the nitrogen lone pair, (ii) the reaction with the nitrogen atom of an endocyclic or exocyclic amine proceeds first by the formation of the cross-linking C–N bond and then by the cleavage of the C–N aziridine bond and the disappearance of the nitrogen lone pair, and (iii) in case ii, this bond breaking and forming occur before the transition state, which has been correlated to the increased Gibbs enthalpy of activation with respect to the reaction with the nitrogen atom of imine functions.

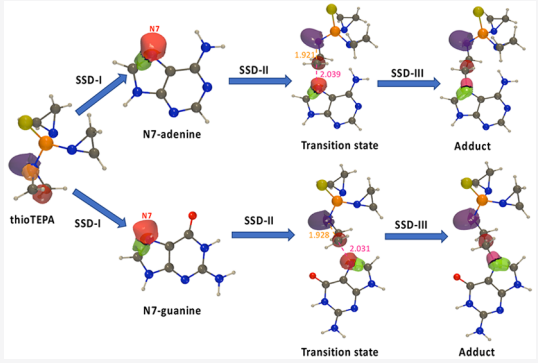

I. INTRODUCTION

Alkylating agents continue to attract much interest owing to their manifold of applications as active pharmaceutical ingredients, laboratory reagents, and mostly potential chemotherapeutics to fight cancer target biochemical processes. These agents act directly on DNA during all phases of the cell cycle by cross-linking the purine base, which induces DNA strand breaks, leads to abnormal base pairing, inhibits cell division, and eventually results in cell death.[1] Unfortunately, because of their systemic toxicity and drug resistance, only a few of these agents are available as palliatives in clinical therapy.[2] *N*,*N*′,*N*″-Triethylenethiophosphoramide (thioTEPA or TT) is an alkylating agent used as an anticancer drug that has been particularly successful for the treatment of ovarian, breast, and bladder cancer.[3,4] Despite its efficiency, thioTEPA was not used extensively because myelosuppression was occasionally severe. However, a renewed interest developed recently where thioTEPA is used in combination with autologous bone marrow transplantation.[5] Moreover, three metabolites of thioTEPA were also found to possess alkylating activity *in vivo*, i.e., TEPA (*N*,*N*′,*N*″-triethylenephosphoramide), monochloroTEPA (*N*,*N*′-diethylene-*N*″-2-chloroethylphosphoramide), and thioTEPA-mercapturate. TEPA as the major metabolite is obtained by cytochrome P450-catalyzed oxidative desulfuration of

Received: February 29, 2020
Revised: April 17, 2020
Published: April 23, 2020

https://dx.doi.org/10.1021/acs.jpca.0c01792
J. Phys. Chem. A 2020, 124, 4068–4080

Scheme 1. ThioTEPA Interaction with Nucleic Acid Bases (Adenine, Guanine) via Two Possible Pathways (Adapted from van Maanen et al.[8])

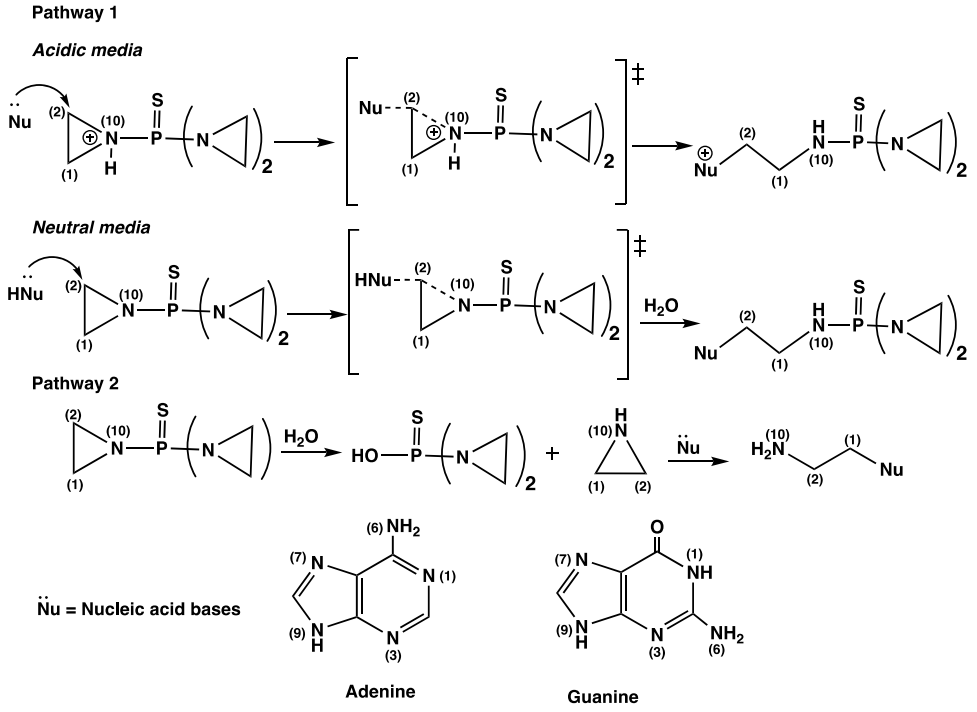

thioTEPA in the liver. ThioTEPA-mercapturate is generated from thioTEPA via the intermediate metabolites monoglutathionylthioTEPA and thioTEPA-cysteinate.[6] Finally, monochloroTEPA can be produced nonenzymatically from TEPA *in vivo* and *in vitro* and its conversion depends strongly on the pH.[7]

The mode of action, the stability, and the reaction mechanism leading to the antitumor activity of thioTEPA have been studied by biochemical and physicochemical methods. For instance, the chemical and the pharmacological analysis of thioTEPA carried out by van Maanen et al.[8] showed that protonation-activated aziridines generated at low pH are rapidly opened in comparison to those in neutral and alkaline environments. Then, by using field ionization mass spectrometry,[9] it has been shown that interactions of nucleic acid bases and thioTEPA gave multiple alkylation possibilities at the N1 position of the thymine, at the N1 or N7 positions of adenine, and at N1 or N7 positions of guanine (see Scheme 1 for the atom labels). Furthermore, Nikolaienko et al.[10] performed a computational chemistry investigation of the complexation of 1−6 molecules of thioTEPA with methylated DNA bases (guanine) at the MP2 (Møller−Plesset second order)/cc-pVTZ level of theory in order to disclose the major physical factors responsible for the high binding affinity of thioTEPA with guanine. They highlighted the role of noncovalent interactions such C−H---H, N−H---N, and C−H---N in the complex stabilization. In addition, molecular docking techniques were able to predict the spatial positions of thioTEPA molecules with respect to the methylated guanine base leading to the alkylation reaction.[10] The hydrolysis of thioTEPA into the thiol form has also been the subject of an electrochemical study showing that the converted amount of thioTEPA into thioTEPA-SH mostly depends on the thioTEPA concentration.[11]

In aqueous solution, the chemical stability of TT is governed by the pH and the temperature. Indeed, it is more stable at 22 °C than at 37 °C and at a pH range of 6−7 rather than at a pH range of 4−5.5. Though several investigations[12,13] have contributed to understanding the reactivity of thioTEPA toward purine bases, particularly guanine, the alkylation mechanism remains unclear because two pathways are possible, as depicted in Scheme 1. In *pathway 1*, thioTEPA cross-links with DNA molecules. This can proceed via two mechanisms, as a function of the pH. At low pH, the ring opening occurs on the protonated aziridine because of its increased ring strain associated with the strengthened electrophilic character. In neutral conditions, the nucleophilic attack occurs directly, without protonation of the aziridinyl group. Alternately, in *pathway 2*, thioTEPA acts as a cell-penetrating carrier for aziridine, which is released via hydrolysis to form cross-links with purine bases.[8]

According to Miller's theory,[14] sites that could interact with electrophilic species are the DNA nucleophilic centers such as the nitrogen atoms of the guanine and adenine purine bases. Despite the chemical similarity of the N7 binding site of guanine and adenine, it is commonly agreed that, *in vivo*, the electrophilic aziridines of TT are the primary targets of nucleophilic attack by N7 of guanine and to a lesser extent by the N3 of adenine.[12] This chemical behavior was ascribed to the molecular shape of guanine compared to adenine (and also cytosine), resulting in stronger steric hindrance in the latter.[15] Indeed, the guanine N7 binding site, exposed in the major groove of normal helical DNA, is more reachable and can thus better react with electrophiles than the N3 of adenine oriented to the minor groove. Still, this cannot totally deny the existence of interactions between thioTEPA and adenine, because van Maanen et al.[8] showed, experimentally, that the reaction between DNA and thioTEPA gives alkylation at both the N7 position of guanine and at the N3 or N7 position of adenine. Therefore, in the present work, we employ density functional theory (DFT) to describe the cross-link mechanism of thioTEPA with guanine and adenine purine bases in physiological conditions, as far as the pH is concerned.

https://dx.doi.org/10.1021/acs.jpca.0c01792
J. Phys. Chem. A 2020, 124, 4068−4080

Following Kim et al.[16] we first performed DFT calculations to confirm the discrimination of the most stable tautomers to react with thioTEPA. Then, considering the presence of several nucleophilic sites, amines and imines, in both adenine and guanine, which may lead to different behaviors toward thioTEPA, the present DFT study focuses in detail on the nucleophilicity of all binding sites in adenine and guanine (N1, N3, N6, N7, and N9) by calculating their reaction and activation energies and by investigating the reaction mechanism. The following questions are addressed: (i) for thioTEPA, is guanine a better nucleophile than adenine, as usually assumed?, (ii) which site(s) of the purine bases are the best nucleophile(s)?, and (iii) how does the electron density reorganize along the reaction pathway? Since the biological activity of the drug is usually tested in aqueous media, the calculations are performed in water, which is modeled as a dielectric continuum. Additional calculations address the role of an explicit water molecule on the cross-linking reaction. Our analysis affords significant details that have not been tackled before such as the kinetics of the addition of adenine and guanine to thioTEPA as well as the details of the reaction mechanisms by resorting to the bond evolution theory (BET). In fact, there are different ways to assess chemical reactivity. One of these is the conceptual DFT (CDFT).[17] It employs relevant chemical descriptors and has been developed and popularized by Paul Geerlings and his collaborators. Here, we resort to quantum chemical topology (QCT) tools,[19] originally introduced by Bader et al.[18,19] as a branch of theoretical and computational chemistry allowing the analysis of dynamical systems through special tools (attractor, basin, gradient path/phase curve, separatrix, critical points), which then leads to valuable information from the wave function of the molecule. In the QCT framework, the BET proposed by Krokidis et al.[20] combines electronic localization functions (ELF)[21,22] with Thom's catastrophe theory (CT)[23] for a better understanding of reaction mechanisms. BET has received growing interest owing to its significance to unravel reaction mechanisms and rationalize the chemical reactivity.[24,25]

The paper is structured in the following manner. In the next section, the key theoretical and computational details are outlined. In the third section, the results on the thermodynamics, kinetics, and mechanisms of the cross-linking reactions at physiological pH are presented and discussed. Finally, we summarize and conclude.

II. THEORETICAL BACKGROUND AND COMPUTATIONAL DETAILS

All calculations were carried out with the aid of the Gaussian09 program package.[26] Molecular geometries of the reactants, intermediates, transition states (TS), and products were fully optimized without any symmetry constraints at the DFT level of approximation using the ωB97X-D[27] functional in combination with the 6-311G++(d,p) basis set. All transition states were subjected, at the same level of approximation, to vibrational frequency calculations to ensure the existence of a single negative eigenvalue of the Hessian, i.e., a single imaginary vibrational frequency, associated with the reaction coordinate. The IRC pathways[28] were traced using the second-order Gonzalez−Schlegel integration method[29,30] in order to check the energy profile connecting each TS to the two associated minima of the proposed mechanism (reactants and intermediates). The polarizable continuum model[31] (PCM) developed by Tomasi's group was used in order to account for implicit solvent effects (water).

The analysis of the reaction mechanisms relies on the calculation of electron localization functions (ELF's), proposed in 1990 by Becke and Edgecombe,[21] to measure the likelihood of finding an electron in the neighborhood space of a reference electron located at a given point and with the same spin. The electron localization function $\eta(r)$ reads

$$\eta(r) = \frac{1}{1 + \left(\frac{D_{\sigma(r)}}{D^0_{\sigma}(r)}\right)^2} \tag{1}$$

The $D_\sigma(r)$ and $D^0_\sigma(r)$ quantities are measures of the electronic localization for ordinary and homogeneous gases, respectively.

$$D_\sigma(r) = \tau_\sigma(r) - \frac{1}{4}\frac{|\nabla\rho_\sigma|^2}{\rho_\sigma(r)} \tag{2}$$

$$D^0_\sigma(\mathrm{r}) = \frac{3}{5}(6\pi)^{2/3}\rho_\sigma{}^{5/3}(r) \tag{3}$$

where $\tau_\sigma(r)$ is defined as the kinetic energy density and $\rho_\sigma(r)$ is the electron density for a given σ spin. The ELF analysis was carried out along the reaction and led to BET pictures, which describe a chemical reaction as a sequence of elementary chemical processes separated by catastrophes. In this definition of a chemical reaction, the catastrophe corresponds to bond formation or bond breaking.

A topological analysis of ELF along the reaction pathway gives attractor basins (domains), in which the probability is maximal for finding an electron pair. The basins can be classified into two types: core and valence basins. The valence basins can be monosynaptic, disynaptic, trisynaptic, and so on, depending on the number of atomic valence shells.[22] The ELF topological analysis of a structure allows characterizing three types of valence basins: protonated basins or V(A, H), monosynaptic basins V(A) corresponding to a nonbonding region, and V(A, B) corresponding to a bonding region.[22] In this paper, we have decided to further subdivide the valence basins between two atoms V(A, B) into three cases in accordance with the Lewis structure: SB(A, B) for single bond, DB(A, B) for double bond, and AB(A, B) for aromatic bond. Furthermore, the monosynaptic basin V(A) that corresponds to a lone pair has been renamed LP(A) while that corresponding to a p lobe is named p(A). For the topological analysis within the BET theory the wave function was obtained for each point of the IRCs, also at the ωB97X-D/6-311G++(d,p) level and the ELF analysis was performed by means of the TopMod package[32] considering a cubic grid with a step size smaller than 0.2 bohr. The ELF basin positions were visualized using the DrawMol and DrawProfile programs.[33,34]

III. RESULTS AND DISCUSSION

III.1. Analysis of Purines Tautomer Forms. The purine bases can adopt several tautomeric forms due to the presence of multiple solvent exchangeable protons. For instance, adenine has the ability to adopt amino/imino tautomeric forms by involving the exocyclic group at the 6-position while guanine has both amino and carbonyl groups and therefore they can exhibit both amino/imino and keto/enol types of tautomerism. Under physiological conditions, the keto and amino forms predominate regarding the imino and enol ones. Therefore, as a first step for establishing the reaction mechanism pathway of thioTEPA with adenine and guanine, the relative electronic energies and Gibbs enthalpies of all their tautomers were evaluated at the

https://dx.doi.org/10.1021/acs.jpca.0c01792
J. Phys. Chem. A 2020, 124, 4068−4080

Scheme 2. Cross-Link Mechanism between thioTEPA and N7 of Adenine/Guanine Purine Bases

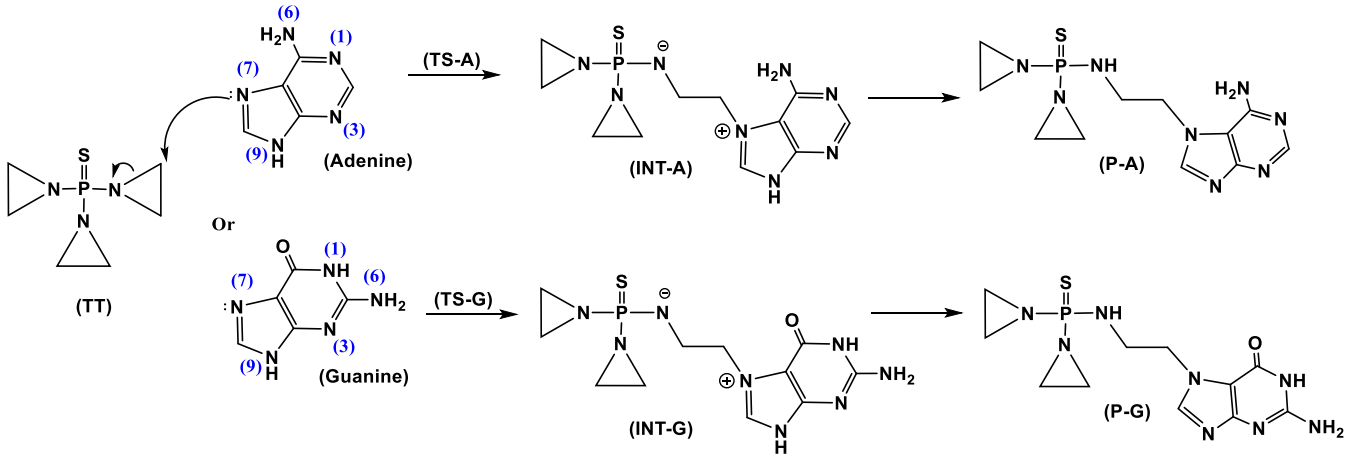

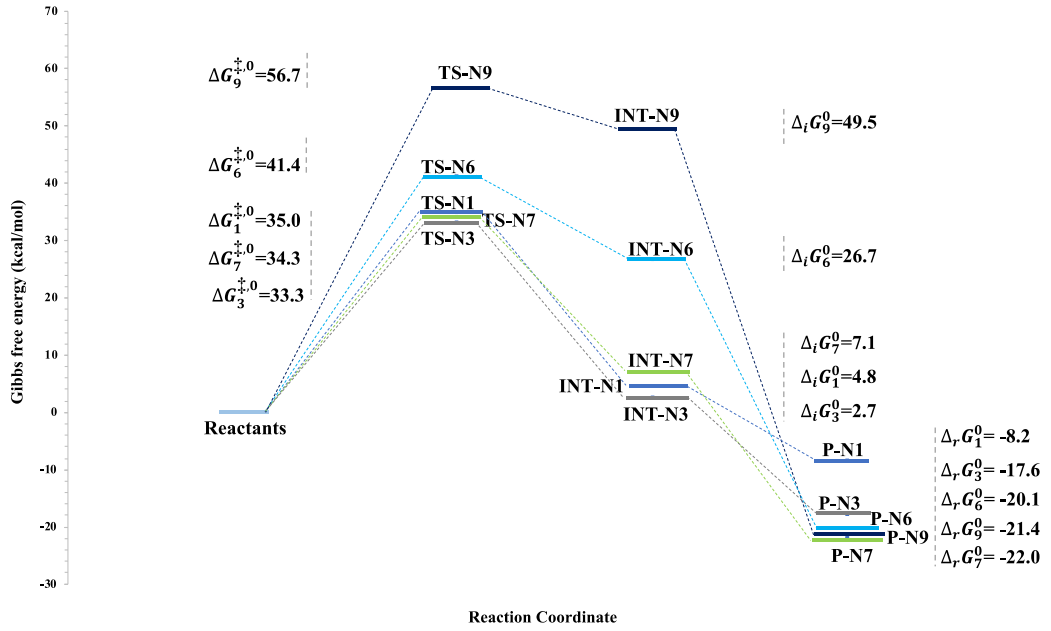

Figure 1. Gibbs free energy profile (kcal/mol) of the addition of adenine to thioTEPA. Calculations were performed at the ωB97X-D/6-311++G(d,p) level by accounting for the solvent (water) effects using IEFPCM.

ωB97X-D/6-311++G(d,p) level of theory in water solvent, as described with IEFPCM (Table S1 and S2 in the Supporting Information). They show an energy range of approximately 19.5 kcal/mol with respect to the most stable tautomer for adenine and 33 kcal/mol for guanine. Thereby, only the most stable entities (T1-A for adenine and T1-G for guanine) have been considered to investigate the interaction mechanism with thioTEPA.

III.2. Thermodynamics and Kinetics of the Adenine and Guanine Nucleophilic Attacks. Scheme 2 displays the cross-link mechanism of thioTEPA with adenine and guanine. Emphasis is put on the N7 binding site, in agreement with experimental findings. The nucleophilic attack of the N7-adenine (N7-guanine) on the electrophilic aziridine ring passes through a transition state, TS-A (TS-G), which is confirmed by the transition vector corresponding to an imaginary frequency of 598i cm^{-1} (586i cm^{-1}), as calculated at the IEFPCM (water)/ωB97X-D/6-311G++(d,p) level of approximation. The corresponding Gibbs enthalpy of activation, $\Delta G^{\ddagger,0}$, attains 34.3 and 35.5 kcal/mol, for these purine bases given in the same order. This attack cleaves the aziridine ring, leading to the formation of a covalent C−N bond and producing an instable zwitterionic intermediate, INT-A (INT-G). The C−N bond length of TS-A (TS-G) amounts to 2.04 Å (2.03 Å), i.e., approximately 0.6 Å longer than in INT-A (INT-G). As shown in Scheme 2, we consider the nucleophilic backside attack trajectory as it has been shown kinetically more favorable regarding the nucleophilic frontside attack.[35,36]

According to the reaction mechanism presented in the Scheme 2, the process takes place via two steps: The first one consists of a S_N2 substitution where the nucleophile is the N7 nitrogen and the leaving group is the ring nitrogen of one of the aziridines. The second step concerns the proton transfer leading to the stabilized neutral product of the reaction. For this step, the inclusion of a water molecule is mandatory in order to allow the proton migration from N9 to the aziridine N10. Thereby, the overall reaction has been investigated in the presence of one explicit water molecule for both adenine and guanine DNA bases (Figures S1 and S2 in the Supporting Information), while the remaining solvent was described at the IEFPCM level.

https://dx.doi.org/10.1021/acs.jpca.0c01792
J. Phys. Chem. A 2020, 124, 4068−4080

Calculations predict low activation barriers for the second step of the reaction, 11.5 and 12.1 kcal/mol for adenine and guanine, respectively. However, the presence of the water molecule only weakly impacts the $\Delta G^{\ddagger,0}$ of the first step of the reaction: 35.1 kcal/mol instead of 34.3 kcal/mol without water molecule for adenine (and 34.8 kcal/mol instead of 35.5 kcal/mol without water molecule for guanine). On the basis of these results, we concentrated on the first step because it is the rate-limiting one and no explicit water molecule was included to investigate its mechanism.

Reaction of Adenine on thioTEPA. For each of the five nucleophilic sites (N1, N3, N7, N6, and N9), the structures and thermodynamic state functions of the stationary and transition states were evaluated at the IEFPCM/ωB97X-D/6-311G++(d,p) level of approximation and led to Gibbs free energy profiles (Figure 1, Table 1). For each case, a conformational analysis was performed because intramolecular interactions could stabilize the structures. This is the case of the H-bonds that can exist between the H atoms of the N6 site ($-NH_2$) or the one of the N9 site ($-NH$) and the aziridine ring N atoms. Calculations reveal that the activation energy is of the order of 34 ± 1 kcal/mol when the N atom belongs to an imine function (N1, N3, and N7) while it strongly increases by about 7 (N6) and 22 (N9) kcal/mol when the nucleophile is an amine. This is a sufficiently large difference to discriminate between the two types of nucleophiles. Experimentally, in the 35−42°C temperature range, activation barriers of 36.8 and 32.9 kcal/mol were determined,[37,38] which is consistent with our values calculated for the attack by an imine function. Calculations also predict a competition between the N3 and N7 binding sites, as well as with N1, with successive differences of Gibbs free energies of activation of only 1 kcal/mol. This result is in agreement with previous studies[39] showing that in addition to the N7-guanine, the N3-adenine targeted aminoethyl adducts are generated by thioTEPA alkylation since the N3 of adenine is exposed in the minor groove. However, when considering the Gibbs free energies of reaction, $\Delta_r G^0$, the most negative values are associated with N9 and N7, leading to the formation of P−N9 and P−N7, respectively. The $\Delta_r G^0$ of the reaction with the N6 (N3) site is 2 (4) kcal/mol higher whereas it is reduced by more than a factor of 2 for the N1 binding site. So, products P−N1, P−N3, and P−N7 are the kinetic products while P−N7 and P−N9 are the thermodynamic ones.

Table 1. Gibbs Free Energies (kcal/mol) of Reaction and Activation for the Reactions between thioTEPA and the Purine Bases as a Function of the Nucleophilic Site[a]

	adenine		guanine	
N reactive site	$\Delta_r G^0$	$\Delta G^{\ddagger,0}$	$\Delta_r G^0$	$\Delta G^{\ddagger,0}$
N1	−8.2	35.0	−15.8	57.7
N3	−17.6	33.3	−13.6	36.2
N6	−20.1	41.4	−19.3	43.7
N7	−22.0	34.3	−19.8	35.5
N9	−21.4	56.7	−19.2	55.2

[a]Calculations were performed at the DFT/ωB97X-D/6-311++G(d,p) level by accounting for the solvent (water) effects using IEFPCM.

The optimized geometries of the thioTEPA-adenine transition states evidence the concerted nucleophilic substitution on the carbon of one of the aziridine moieties by the adenine binding sites (Figure 2). H-bond stabilizations are observed for TS-N1 [d(H--N) = 2.10 Å], TS-N3 [d(H--N) = 1.95 Å], and TS-N7 [d(H--N) = 2.08 Å], with the smallest N---H distance corresponding to the lowest activation energy. All transition states were further validated by tracing the reaction pathway carrying out intrinsic reaction coordinate (IRC) calculations. The IRCs highlight the simultaneous attack of the nitrogen atom of adenine and the departure of the N atom of the aziridine ring as a leaving group. The imaginary frequencies of the corresponding vibrations amount to 616i cm^{-1} for N1, 612i cm^{-1} for N3, 598i cm^{-1} for N7, 623i cm^{-1} for N6, and 608 cm^{-1} for N9.

Reaction of Guanine on thioTEPA. The same reactions were then investigated with guanine as nucleophilic agent (Figure 3, Table 1). Like for adenine, smaller activation Gibbs free enthalpies characterize the attack by an imine (N3 and N7) than by an amine function (N1, N6, and N9). Indeed, when the nucleophile is an amine function, the $\Delta G^{\ddagger,0}$ values are 8−22 kcal/mol higher. Then, contrary to adenine, the attack by N7 has a slightly smaller activation Gibbs free enthalpy (by 0.7 kcal/mol) than by N3, again showing the competition between the two sites. Considering the lowest $\Delta G^{\ddagger,0}$ value of each purine base, the reaction with an adenine (N3 site) is favored over the reaction with a guanine (N7 site) by 2.2 kcal/mol. Looking at the Gibbs free energies of the reaction, the smallest value is obtained for the N7 site, followed closely by N6 and N9. So, the reaction with N7 gives the kinetic and thermodynamic products. In the case of N1 and N3, the $\Delta_r G^0$ values are 4 and 6 kcal/mol higher, respectively. In comparison to the reaction with adenine, the $\Delta_r G^0$ values are less negative, in parallel with more positive $\Delta G^{\ddagger,0}$ values. In conclusion, this agrees with the *in vitro* studies showing the preference for interaction with the N7 binding site of both adenine and guanine.

Among the transition states, only TS-N3 presents a stabilizing H-bond, as evidenced by the optimized geometries [d(H--N) = 2.06 Å] (Figure 4). The imaginary vibrational frequencies are generally slightly smaller than in the adenine case (594i cm^{-1} for N1, 601i cm^{-1} for N3, 586i cm^{-1} for N7, 613i cm^{-1} for N6, and 611i cm^{-1} for N9).

III.3. Mechanistic Study of the Adenine and Guanine Nucleophilic Attacks. To unravel the mechanism of the attacks of thioTEPA by adenine or guanine, BET analyses were conducted for the different imine and amine reaction sites. The emphasis is put first on the N7 sites of both guanine and adenine so that the results on N1, N3, N6, and N9 are given in the Supporting Information. For each BET analysis, we only report those basins with an evolving electron population along the IRC. Scheme 3 introduces the labeling for the different atoms of thioTEPA, guanine, and adenine as used in the BET analysis.

BET Analysis for the Attack of the N7 Binding Site of Adenine on thioTEPA. The formation of the cross-link between thioTEPA and adenine takes place in three structural stability domains (SSDs). The evolution of the ELF basins and their electron population are shown in Figures 5 and 6 while Figure 7 sketches the basins on the Lewis structures.

In the SSD-I, five basins of the reactants are highlighted, i.e., (i) the monosynaptic basins associated with the lone pairs (LPs) of the N7 [LP(N7), with about 3.0e] and N10 [LP(N10) with about 2.5e] nitrogen atoms, (ii) the disynaptic basins of two single bonds, SB(C1,N10) and SB(C1,C2) with populations of about 1.4e and 2.0e, respectively, and (iii) the disynaptic basin AB(N7,C8) of the aromatic bond between C8 and N7 having a population close to 3.0e (Figure 5). At the beginning of SSD-II, the SB(C1,N10) basin disappears while the electron population of LP(N10) increases by 1.5 units. This corresponds to the

https://dx.doi.org/10.1021/acs.jpca.0c01792
J. Phys. Chem. A 2020, 124, 4068−4080

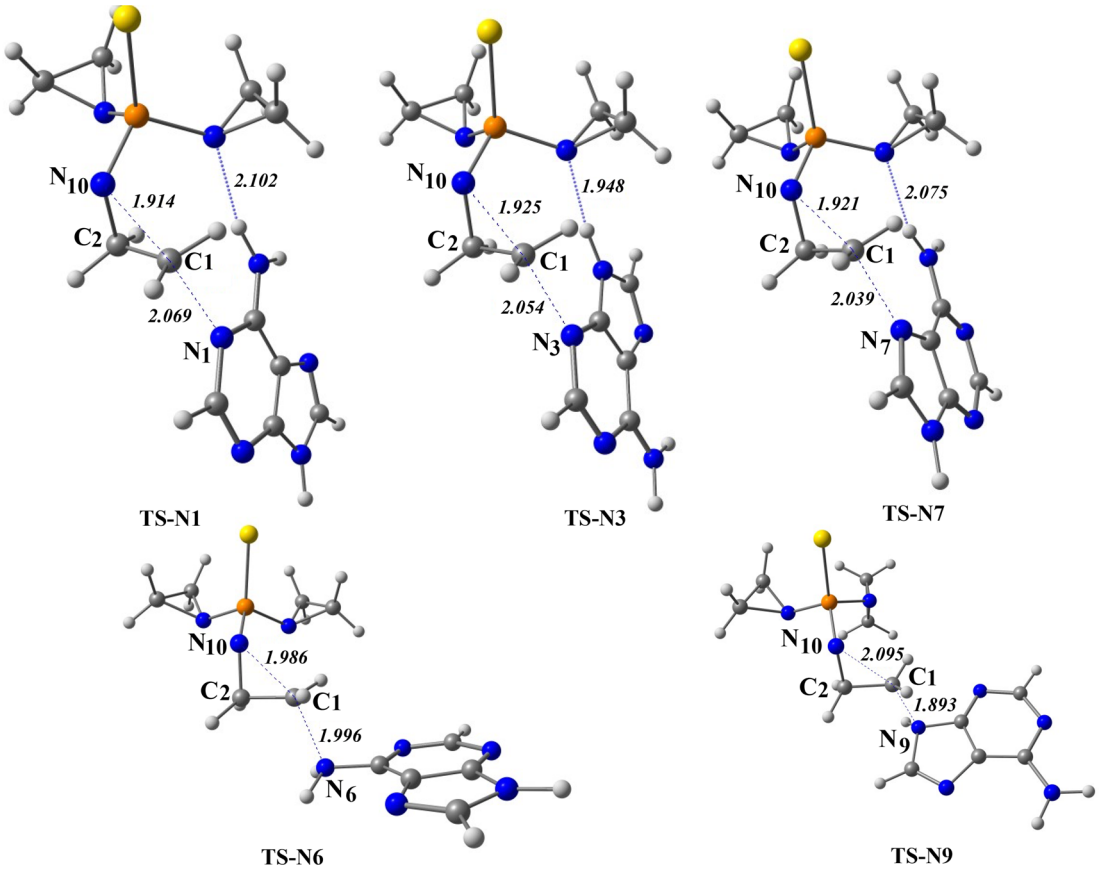

Figure 2. Optimized geometries of the thioTEPA−adenine transition states as predicted at the ωB97X-D/6-311++G(d,p) level of theory using IEFPCM to describe solvent (water) effects.

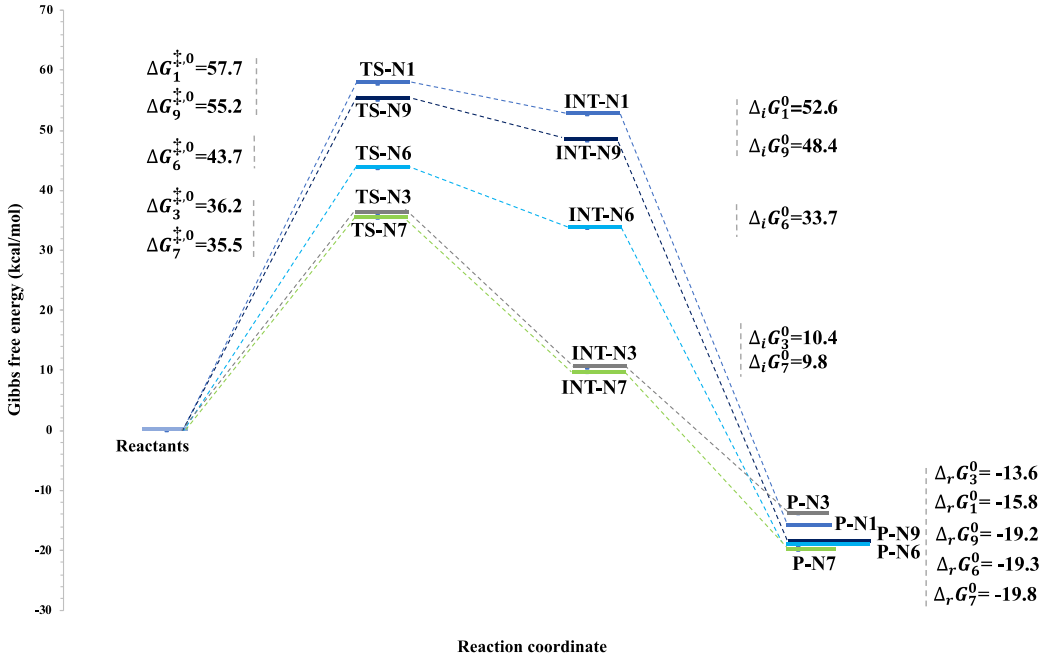

Figure 3. Gibbs free energy profile (kcal/mol) of the addition of guanine to thioTEPA. Calculations were performed at the ωB97X-D/6-311++G(d,p) level by accounting for the solvent (water) effects using IEFPCM.

breaking of the C1—N10 bond and the transfer of its electrons to the lone pair of N10. Within SSD-II, the population of LP(N7) decreases by about 0.5*e*, which anticipates the appearance of the new SB(C1,N7) disynaptic basin. In addition, the population of SB(C1,C2) attains a maximum for a geometry close to the TS before returning almost to its initial value. In the SSD-III domain, the LP(N7) monosynaptic basin is converted into the disynaptic basin SB(C1,N7) (with a population of 1.9 *e*)

https://dx.doi.org/10.1021/acs.jpca.0c01792
J. Phys. Chem. A 2020, 124, 4068−4080

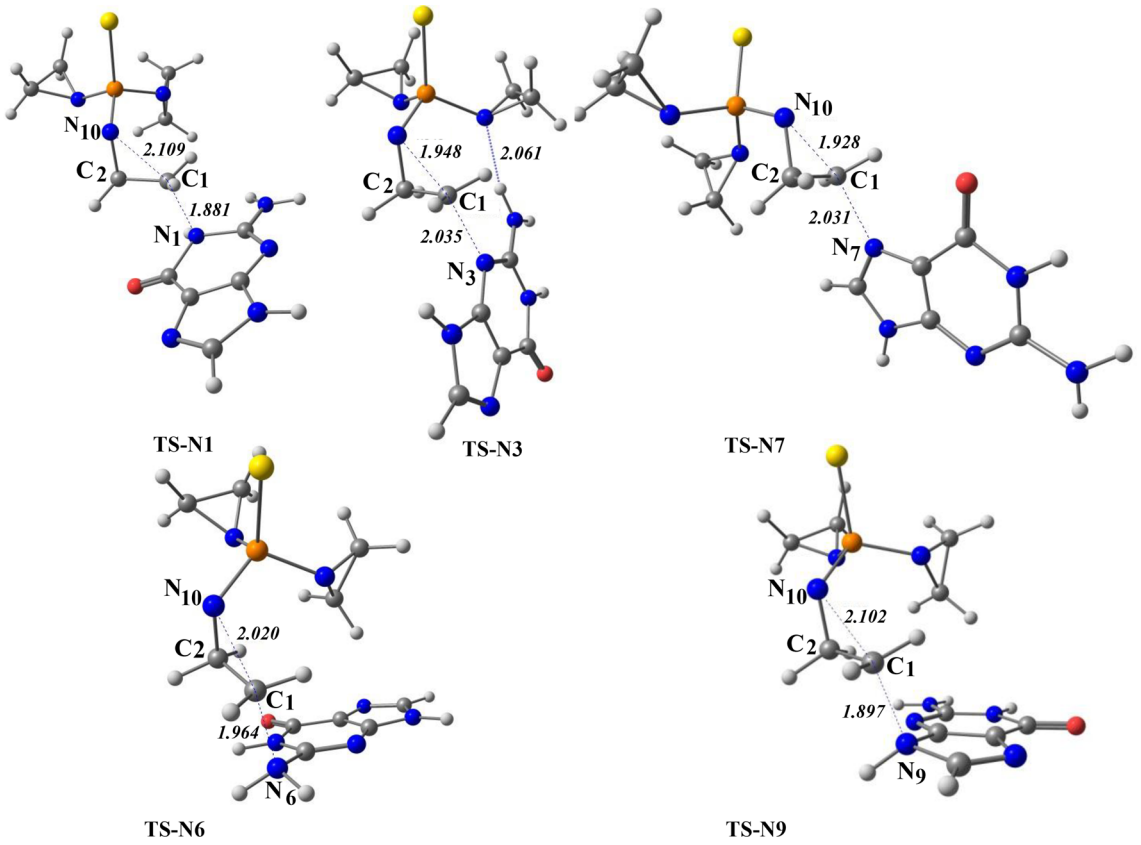

Figure 4. Optimized geometries of the thioTEPA−guanine transition states as predicted at the ωB97X-D/6-311++G(d,p) level of theory using IEFPCM to describe solvent (water) effects.

Scheme 3. Labeling of the N and H Atoms of thioTEPA, Guanine, and Adenine Used in the BET Analysis

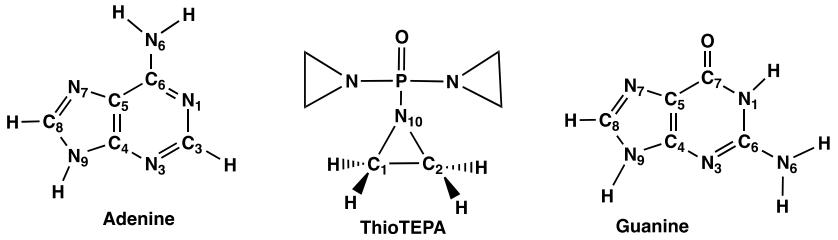

which indicates the formation of a single bond between C1 and N7 from the lone pair on the N7 atom as sketched in the Lewis structures (Figure 7). Simultaneously, the population of the AB(N7,C8) basin increases from 2.8*e* to 3.6*e*. This originates from the fact that the C8 ═N7 aromatic bond takes back some electron population from the N7 lone pair that was previously shared due to its delocalization. At the end of the IRC, out of the initially considered basins, four basins are present, i.e., (i) the monosynaptic LP(N10) with a population close to 3.8*e* and (ii) three disynaptic basins of the SB(C1,C2) (∼2.0*e*), SB(C1, N7) (∼2.0*e*), and AB(N7,C8) (∼3.5*e*) bonds.

BET Analysis for the Attack of the N7 Binding Site of Guanine on thioTEPA. The BET analysis for the attack of the N7 site of guanine on thioTEPA (Figures 8−10) shows a similar electron evolution along the IRC path to the one observed with N7 of adenine. So, the analysis highlights three SSDs. In the first domain (SSD-I), the ELF basins of the reactants and their electron populations vary little with (i) the LP(N7) and LP(N10) monosynaptic basins with electron populations of 2.8*e* and 2.5*e*, respectively, (ii) a SB(C1,N10) disynaptic basin that shows a decrease of population from 1.4*e* to 1.1*e* at the end of SSD-I, (iii) the disynaptic basin SB(C1,C2) (1.9*e*), and (iv) the disynaptic basin AB(N7,C8) with an electron population of 2.8*e*. The SSD-II is characterized by an increase, by about 1.5*e*, of the electron population for the monosynaptic basin LP(N10), resulting from the electron transfer from the SB(C1,N10) basin that corresponds to the breaking of the C1−N10 bond. Like in the case of adenine, it is accompanied by an increase of the population of the disynaptic SB(C1,C2) basin close to the TS maximum. Then, the SSD-III domain is characterized (i) by the disappearance of the monosynaptic LP(N7) basin that is transformed into the SB(C1,N7) basin and then (ii) by the simultaneous increase of the population of the AB(N7,C8) basin. Again, this shows that a part of the π electrons, shared with the LP(N7), is now taken back. We end up the IRC with the same basins having nearly identical electron population as in the N7 adenine case.

BET Analysis for the Attack by Other Binding Sites of Adenine and Guanine on thioTEPA. The corresponding BET analyses were performed for the other binding sites of adenine

https://dx.doi.org/10.1021/acs.jpca.0c01792
J. Phys. Chem. A 2020, 124, 4068−4080

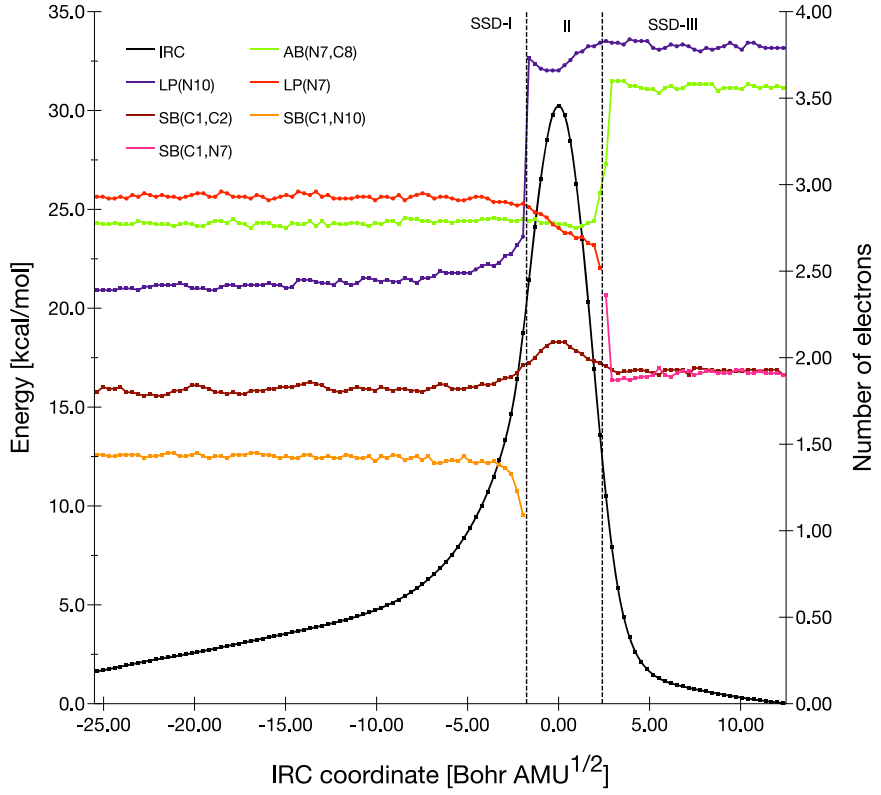

Figure 5. Electron populations (e) evolution for selected basins along the IRC of the reaction between adenine (N7) and thioTEPA as determined at the IEFPCM(water)/ωB97X-D/6-311G++(d,p) level of approximation. These evolutions are plotted on top of the potential energy surface.

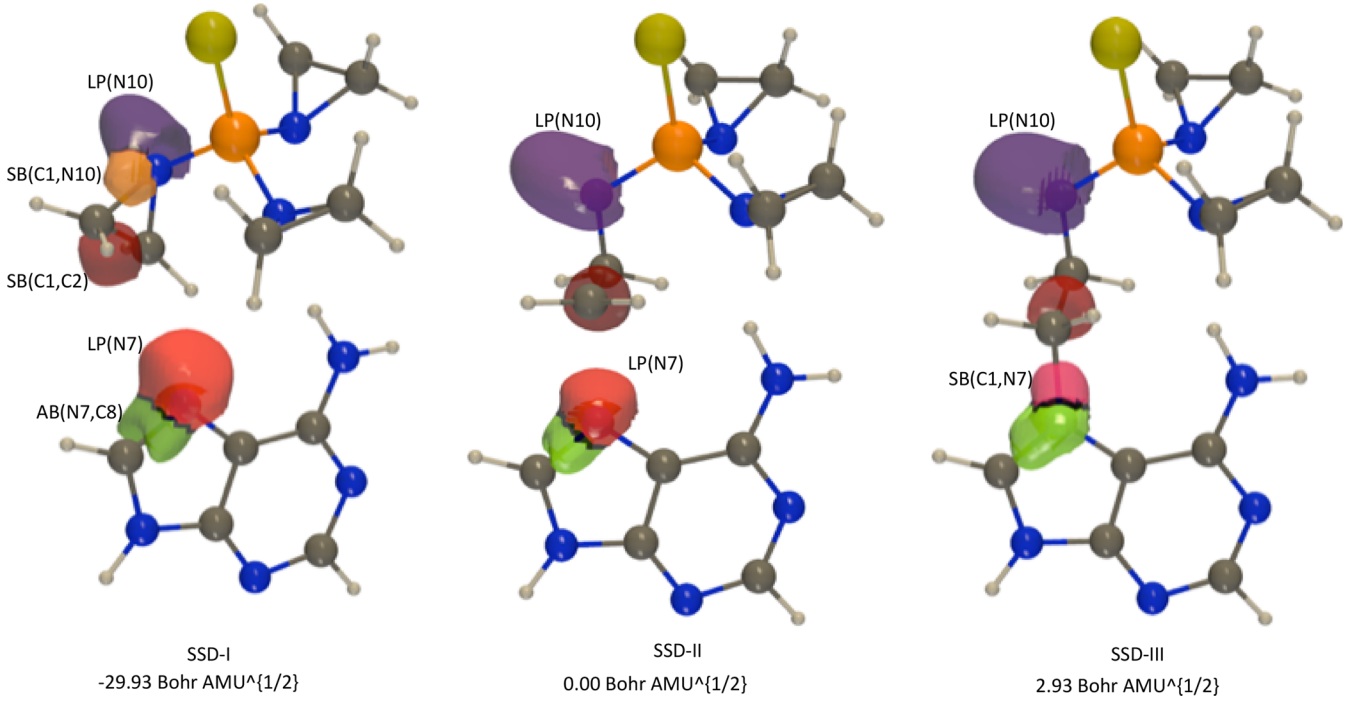

Figure 6. ELF basin isosurfaces for selected points that are representative of each of the SSDs found along the IRC corresponding to the transition state of the reaction between the N7 of adenine and thioTEPA and its reaction coordinate. See Figure 5 for the color labeling of the basins.

and guanine and they are presented in Figures S3−S10 and S11−S18, respectively. We highlight here the key features and major differences with respect to the attack by the N7 sites. Among these, when looking to the Lewis structures (Scheme 1), we notice that the nitrogen attack sites differ by the nature of the binding site function (amine versus imine) and, furthermore, by the type of amine (exocyclic versus endocyclic). At least three types of sites can be defined: imine sites (N1 adenine, N3

https://dx.doi.org/10.1021/acs.jpca.0c01792
J. Phys. Chem. A 2020, 124, 4068−4080

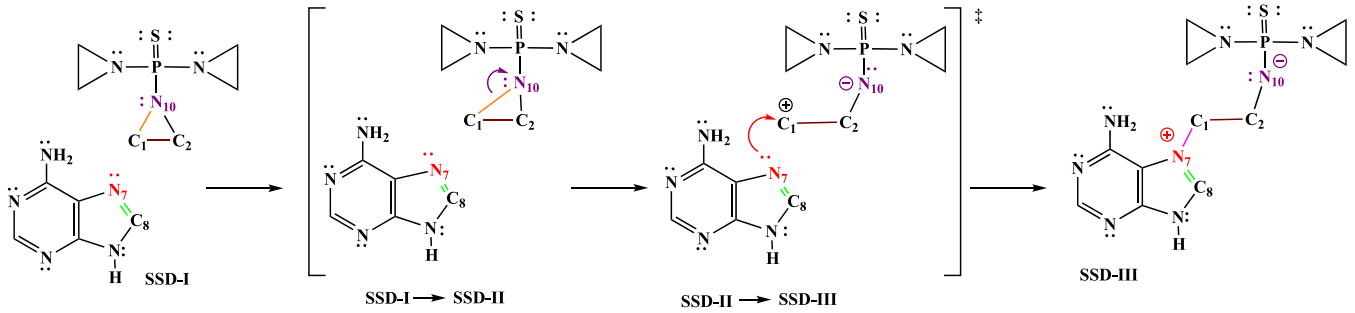

Figure 7. Lewis structures along the IRC of the reaction between adenine N7 and thioTEPA.

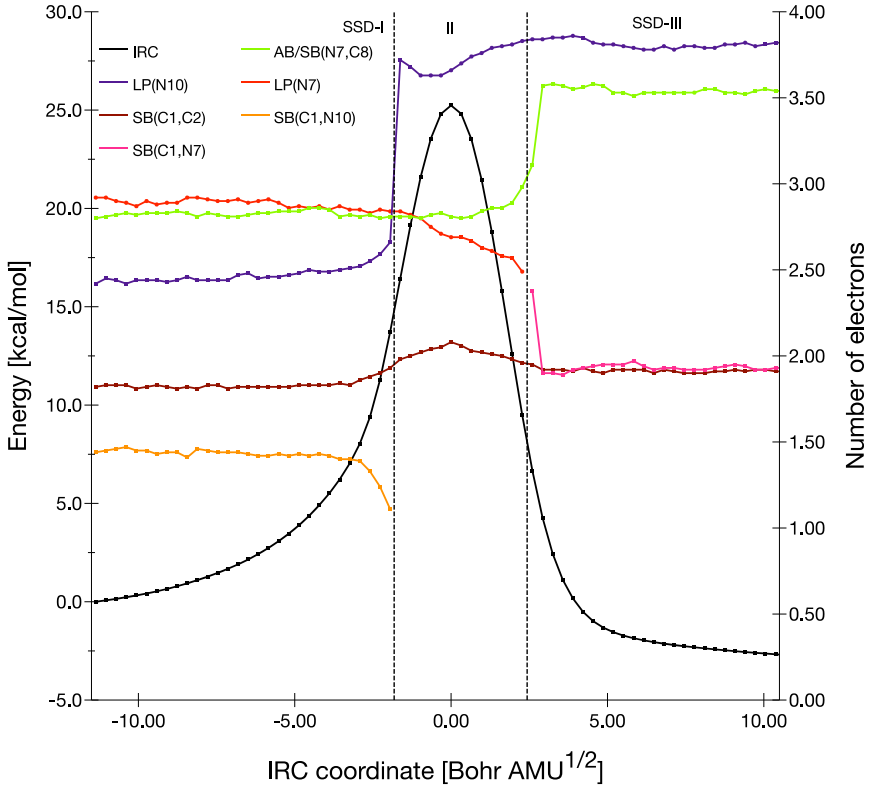

Figure 8. Electron populations (e) evolution for selected basins along the IRC of the reaction between guanine (N7) and thioTEPA as determined at the IEFPCM(water)/ωB97X-D/6-311G++(d,p) level of approximation. These evolutions are plotted on top of the potential energy surface.

adenine, N7 adenine, N3 guanine, N7 guanine), endocyclic secondary amine (N9 adenine, N1 guanine, N9 guanine), and exocyclic primary amine (N6 adenine, N6 guanine). In addition, for the imine sites, the position of the ($-NH_2$) group in α or γ position to the imine site influences the BET analysis.

When the nucleophile is the N1 of adenine (imine with NH_2 in α position, Figures S3 and S4), the BET analysis is comparable to the one of the N7-adenine site: the rupture of the C1−N10 bond and the transfer of its electron population to the lone pair of N10 (SSD-II) happen before the attack of the lone pair of N1 on the C1 to form the SB(C1,N1) basin (SSD-III). However, the presence of the ($-NH_2$) in the α position has two effects: (i) a new basin p(N1) ($\simeq 1$ e) appears and (ii) the electron population of the LP(N6) basin decreases slightly while the one of the AB(C6,N6) basin increases slightly along the IRC. These effects can be explained by the resonance structures where the lone pair on the amino group is delocalized to compensate the positive charge on atom N1 (Scheme S1).

In the case of an attack by the N3 atom of adenine (imine with NH_2 in γ position, Figures S5 and S6), the BET analysis is again comparable to the one of the N7-adenine site. In addition, similarly to the N1-adenine case, the presence of the amino group, here in the γ position, is highlighted on the BET analysis by the decrease of the electron population of the LP(N6) basin and the slight increase of the electron population of the basins AB(C6,N6) and AB(N1,C3). Nevertheless, contrary to the N1-adenine case, the amino group is too far away to create a new p(N3) basin. From the resonance structures (Scheme S1), we observe that the positive charge on the nitrogen is delocalized between the two amino N atoms, N3 and N6 (of NH_2).

Turning now to the case where the nitrogen (N6) of an exocyclic primary amine function attacks thioTEPA (Figures S7 and S8), the attack of the lone pair of N6 on the C1 to form the SB(C1,N6) basin (SSD-II) happens before the rupture of the C1−N10 bond and the transfer of its electron population to the lone pair of N10 (SSD-IV), contrary to the previous cases. This

https://dx.doi.org/10.1021/acs.jpca.0c01792
J. Phys. Chem. A 2020, 124, 4068−4080

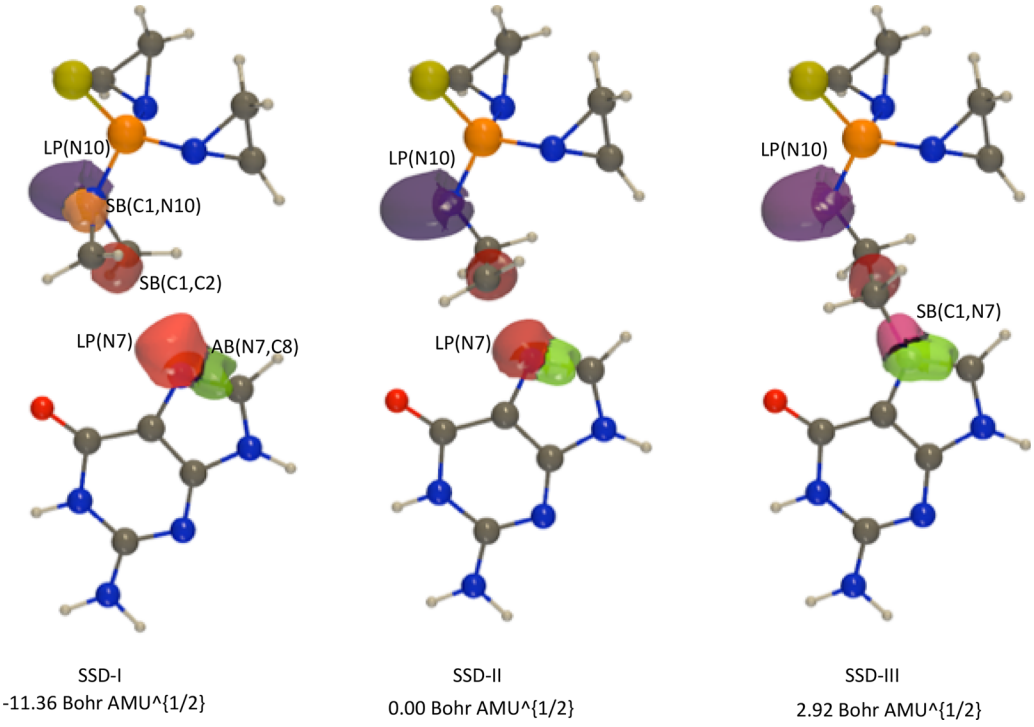

Figure 9. ELF basin isosurfaces for selected points that are representative of each of the SSDs found along the IRC corresponding to the transition state of the reaction between the N7 of guanine and thioTEPA and its reaction coordinate. See Figure 8 for the color labeling of the basins.

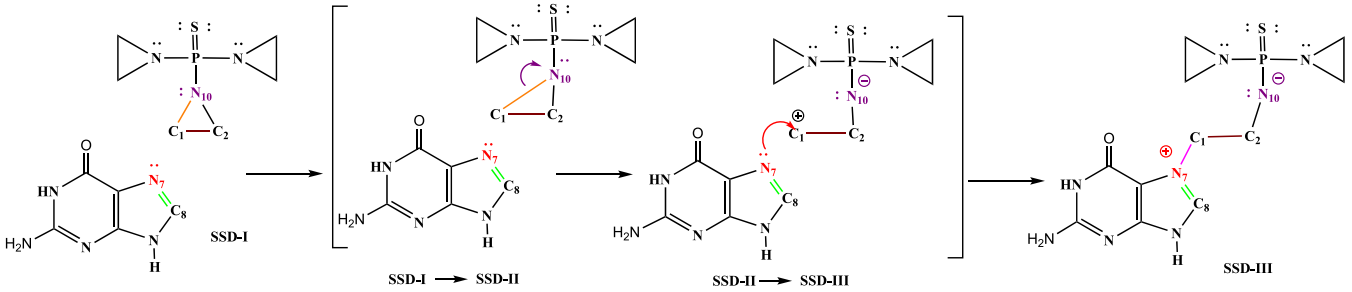

Figure 10. Lewis structures along the IRC of the reaction between guanine N7 and thioTEPA.

behavior is correlated to the higher activation energies associated with this site, as discussed in the section above. In addition, during the transfer of electron population between the LP(N6) basin toward the SB(C1,N6) basin, the N pyramidal shape is inverted (the NH_2−C6 is perfectly planar when both basin populations are identical [at 4.97 bohr $AMU^{1/2}$], Figure S8). In the meantime, the electron population of the AB(C6,N6) basin changes from ≃2.5*e* to ≃2.0*e* to become SB(C6,N6). Indeed, in adenine as a reactant, the NH_2 group can be considered as aromatic (the lone pair is delocalized and the group is in the molecular plane), while in the product, the lone pair has been transformed into a bond and therefore is no more delocalized into the C6−N6 bond (Figure S8, Scheme S1).

When the attack is made by the N9 of the endocyclic secondary amine function (Figures S9 and S10), the attack of the lone pair of N9 on the C1 to form the SB(C1,N9) basin (SSD-II) and the rupture of the C1−N10 bond and the transfer of its electron population to the lone pair of N10 (SSD-III) happen nearly simultaneously. Again, this behavior can be correlated to the higher activation energies associated with this site, as discussed in the section above. The BET analysis is similar to the previous exocyclic amine case with one noticeable difference: at the beginning of SSD-II, we do not observe the N pyramidal inversion together with the transfer of electron population between the LP(N9) basin toward the SB(C1,N9) basin since the NH group is endocyclic and is already planar. Therefore, we observe instead the disappearance of the LP(N9) basin and the creation at the same time of the SB(C1,N9) basin. Similarly to the previous case, in SSD-III the AB(C8,N9) basin changes from ≃2.3*e* to ≃2.0*e* to become SB(C8,N9) (Figure S10, Scheme S1). Indeed, the five-membered ring loses its aromaticity since N9 becomes a ternary amine cation. As a consequence, the AB(N7,C8) basin is also transformed and becomes more of a double bond (slight increase of its electron population).

In the case of the attack of thioTEPA by the nitrogen atoms of endocyclic secondary amine functions of guanine N1 and N9 (Figures S11 and S12 and Figures S17 and S18), the BET profiles are very similar to those observed for N9 of the adenine. They also highlight that the attack of the lone pair of N1/N9 on the C1 to form the SB(C1,N1/N9) basin (SSD-II) and the rupture of the C1−N10 bond and the transfer of its electron population to the lone pair of N10 (SSD-II) happen nearly simultaneously. Like for adenine N1 (Figures S3 and S4), the N3 of guanine (Figures S13 and S14) belongs to an imine function

https://dx.doi.org/10.1021/acs.jpca.0c01792
J. Phys. Chem. A 2020, 124, 4068−4080

with NH_2 in α position. The BET analysis therefore slightly differs from the N7 attack and from the adenine N3 (where the NH_2 group is in γ position) by the presence of a new basin p(N3) ($\simeq$1.5 *e*, SSD-III). Similarly to adenine N1 (Figures S3 and S4), we also observe that the electron population of the LP(N6) basin decreases slightly while the one of the AB(C6,N6) basin increases slightly along the IRC. These effects can be explained by the resonance structures where the lone pair on the amino group is delocalized to compensate the positive charge on atom N3 (Scheme S2). The only small difference with respect to adenine N1 is the fact that the bond N3−C4 in guanine is a single bond while in adenine, the corresponding bond N1−C3 is aromatic (Schemes S1 and S2). On the BET analysis, this is highlighted by the electron population of SB(N3,C4) and p(N3) in guanine N3 (Figure S13) that approximatively amount to 2.0*e* and 1.5*e*, respectively, while the corresponding basins in adenine N1 (Figure S3), AB(N1,C3) and p(N1) have an electron population of approximatively 2.5*e* and 1.0*e*, respectively. Finally, the nucleophile attack of thioTEPA by the nitrogen (N6) of the exocyclic primary amine function of guanine provides a BET profile (Figures S15 and S16) similar to that observed for the analogous N6 atom of adenine (Figures S7 and S8).

IV. CONCLUSIONS

The reactions of the adenine and guanine purine bases on *N*,*N*′,*N*″-triethylenethiophosphoramide (thioTEPA), an alkylating agent used as anticancer drug, has been investigated at the density functional theory level of approximation, using a range-separated exchange−correlation functional including London dispersion corrections, ωB97X-D. These cross-linking reactions are studied for each of their five nitrogen atoms, which all present a nucleophilic character, of the most stable tautomers of adenine and guanine. Solvent effects have been accounted for by using the polarizable continuum model, considering water as solvent and mimicking the physiological pH conditions. The whole reaction is decomposed into a nucleophilic addition and a proton "migration" that is mediated by the solvent molecules. Calculations have revealed that the first step is rate determining, that the proton migration is almost barrierless, and that the presence of a water molecule to mediate the proton migration has a negligible role on the kinetics of the first step. The first step has therefore been characterized in more detail showing (i) the activation energy (Gibbs free enthalpy) is smaller for imine nitrogen atoms than amine nitrogen atoms, (ii) for the imine functions, the activation energy is slightly smaller for adenine than guanine and that the reaction energy is also slightly in favor of the alkylation by adenine, and (iii) among the amine nitrogen atoms, the exocyclic one is associated with a smaller activation energy than the endocyclic one, owing to the transition state stabilization by a hydrogen bond. These results agree to some extent with experimental *in vivo* observations, i.e., concerning the stronger reactivity of the imine functions with respect to the amine ones but not about the difference of reactivity of adenine and guanine, impacted by the *in vivo* surrounding that is not accounted for in our modeling. Further details of the reaction mechanisms have then been unraveled by employing the bond evolution theory, combining the use of electronic localization functions, and their evolution along the intrinsic reaction coordinate, with Thom's catastrophe theory. These analyses, suitable for highlighting the populations of the major monosynaptic and disynaptic basins, have revealed (i) the reaction with imine nitrogen atoms begins by the cleavage of the C−N aziridine bond and is followed by the simultaneous formation of the new C−N bond and the disappearance of the nitrogen lone pair, (ii) the reaction with the nitrogen atom of an endocyclic or exocyclic amine proceeds first by the formation of the cross-linking C−N bond and then by the cleavage of the C−N aziridine bond and the disappearance of the nitrogen lone pair, and (iii) in the latter case, these bond breaking and forming occur before the transition state, which has been correlated with the increased Gibbs enthalpy of activation with respect to the reaction with the nitrogen of imine functions.

■ ASSOCIATED CONTENT

Supporting Information

The Supporting Information is available free of charge at https://pubs.acs.org/doi/10.1021/acs.jpca.0c01792.

Tables with the relative electronic energies and Gibbs enthalpies of the adenine and guanine tautomers; mechanism and Gibbs enthalpy diagrams for the reaction of thioTEPA with adenine/guanine mediated by one explicit water molecule; Lewis structures along the IRC of the reaction between adenine/guanine and thioTEPA; BET analysis for the attack by the N1, N3, N6, and N9 binding sites of adenine/guanine on thioTEPA (population evolutions and ELF basin isosurfaces) (PDF)

■ AUTHOR INFORMATION

Corresponding Authors

Benoît Champagne − *Laboratory of Theoretical Chemistry (LCT) and Namur Institute of Structured Matter (NISM), University of Namur, B-5000 Namur, Belgium;* orcid.org/0000-0003-3678-8875; Email: benoit.champagne@unamur.be

Vincent Liégeois − *Laboratory of Theoretical Chemistry (LCT) and Namur Institute of Structured Matter (NISM), University of Namur, B-5000 Namur, Belgium;* orcid.org/0000-0003-2919-8025; Email: vincent.liegeois@unamur.be

Authors

Emna Cherni − *Chemistry Department, Faculty of Sciences of Tunis, University of Tunis El Manar, 2092 Tunis, Tunisia; Laboratory of Materials Molecules and Applications Preparatory Institute for Scientific and Technical Studies, Carthage University, 2075 Tunis, Tunisia; Laboratory of Theoretical Chemistry (LCT) and Namur Institute of Structured Matter (NISM), University of Namur, B-5000 Namur, Belgium*

Abel Idrice Adjieufack − *Laboratory of Theoretical Chemistry (LCT) and Namur Institute of Structured Matter (NISM), University of Namur, B-5000 Namur, Belgium; Physical and Theoretical Chemistry Laboratory, University of Yaoundé 1, Yaoundé, Cameroon*

Manef Abderrabba − *Laboratory of Materials Molecules and Applications Preparatory Institute for Scientific and Technical Studies, Carthage University, 2075 Tunis, Tunisia*

Sameh Ayadi − *Laboratory of Materials Molecules and Applications Preparatory Institute for Scientific and Technical Studies, Carthage University, 2075 Tunis, Tunisia*

Complete contact information is available at: https://pubs.acs.org/10.1021/acs.jpca.0c01792

Notes

The authors declare no competing financial interest.

[#]E.C. and A.I.A. contributed equally to this work.

https://dx.doi.org/10.1021/acs.jpca.0c01792
J. Phys. Chem. A 2020, 124, 4068−4080

■ ACKNOWLEDGMENTS

This work is dedicated to Prof. Paul Geerlings at the occasion of his 70th birthday. In Belgium and around the world, Paul is recognized as a gentleman theoretical chemist who is continuing fostering the noble use of computational and theoretical chemistry to have insights into the chemical phenomena. This work has been supported by the Tunisian Ministry of Higher Education and Scientific Research and the University of Namur for a short-term visit of E.C. at UNamur. A.I.A. thanks the University of Namur (Belgium) for his UNamur-CERUNA Ph.D. Mobility Fellowship. V.L. thanks the F.R.S.-FNRS for his Research Associate position. The calculations were performed on the computers of the Consortium des Équipements de Calcul Intensif (CÉCI, http://www.ceci-hpc.be) and particularly those of the Technological Platform of High-Performance Computing, for which the authors gratefully acknowledge the financial support of the FNRS-FRFC, of the Walloon Region, and of the University of Namur (Conventions No. 2.5020.11, GEQ U.G006.15, 1610468, and RW/GEQ2016).

■ REFERENCES

(1) Torgovnick, A.; Schumacher, B. DNA Repair Mechanisms in Cancer Development and Therapy. *Front. Genet.* **2015**, *6*, 157.
(2) Baik, M.-H.; Friesner, R. A.; Lippard, S. J. Theoretical Study of Cisplatin Binding to Purine Bases: Why does Cisplatin prefer Guanine over Adenine? *J. Am. Chem. Soc.* **2003**, *125*, 14082−14092.
(3) Van der Wall, E.; Beijnen, J. H.; Rodenhuis, S. High-Dose Chemotherapy Regimens for Solid Tumors. *Cancer Treat. Rev.* **1995**, *21*, 105−132.
(4) Kondo, E.; Ikeda, T.; Goto, H.; Nishikori, M.; Maeda, N.; Matsumoto, K.; Kitagawa, H.; Noda, N.; Sugimoto, S.; Hara, J. Pharmacokinetics of Thiotepa in High-Dose Regimens for Autologous Hematopoietic Stem Cell Transplant in Japanese Patients with Pediatric Tumors or Adult Lymphoma. *Cancer Chemother. Pharmacol.* **2019**, *84*, 849−860.
(5) O'Dwyer, P. J.; LaCreta, F.; Engstrom, P. F.; Peter, R.; Tartaglia, L.; Cole, D.; Litwin, S.; DeVito, J.; Poplack, D.; DeLap, R. J. Phase I/Pharmacokinetic Reevaluation of Thiotepa. *Cancer Res.* **1991**, *51*, 3171−3176.
(6) Li, F.; Patterson, A. D.; Höfer, C. C.; Krausz, K. W.; Gonzalez, F. J.; Idle, J. R. A Comprehensive Understanding of Thiotepa Metabolism in the Mouse Using UPLC−ESI-QTOFMS-Based Metabolomics. *Biochem. Pharmacol.* **2011**, *81*, 1043−1053.
(7) Cohen, B. E.; Egorin, M. J.; Nayar, M. S.; Gutierrez, P. L. Effects of pH and Temperature on the Stability and Decomposition of N, N′ N ″-triethylenethiophosphoramide in Urine and Buffer. *Cancer Res.* **1984**, *44*, 4312−4316.
(8) van Maanen, M. J.; Smeets, C. J.; Beijnen, J. H. Chemistry, Pharmacology and Pharmacokinetics of N, N′, N″-triethylenethiophosphoramide (Thiotepa). *Cancer Treat. Rev.* **2000**, *26*, 257−268.
(9) Sukhodub, L. F.; Shelkovsky, V. S.; Kosevich, M. V.; Pyatigorskaya, T. L.; Zhilkova, O. Y. Nucleic Acid Base Complexes with Thiotepa as Revealed by Field Ionization Mass Spectrometry. *Biol. Mass Spectrom.* **1986**, *13*, 167−170.
(10) Nikolaienko, T. Y.; Bulavin, L. A.; Sukhodub, L. F. The Complexation of the Anticancer Drug ThioTEPA with methylated DNA Base Guanine: Combined Ab initio and QTAIM Investigation. *Mol. Inf.* **2014**, *33*, 104−114.
(11) Marín, D.; Valera, R.; La Red, E. de; Teijeiro, C. Electrochemical Study of Antineoplastic Drug Thiotepa Hydrolysis to Thiol Form and Thiotepa-DNA Interactions. *Bioelectrochem. Bioenerg.* **1997**, *44*, 51−56.
(12) Kheffache, D.; Ouamerali, O. Some Physicochemical Properties of the Antitumor Drug Thiotepa and its Metabolite Tepa as Obtained by Density Functional Theory (DFT) Calculations. *J. Mol. Model.* **2010**, *16*, 1383−1390.
(13) Torabifard, H.; Fattahi, A. DFT Study on Thiotepa and Tepa Interactions with their DNA Receptor. *Struct. Chem.* **2013**, *24*, 1−11.
(14) Benigni, R.; Bossa, C. Mechanisms of Chemical Carcinogenicity and Mutagenicity: A Review with Implications for Predictive Toxicology. *Chem. Rev.* **2011**, *111*, 2507−2536.
(15) La, D. K.; Swenberg, J. A. DNA Adducts: Biological Markers of Exposure and Potential Applications to Risk Assessment. *Mutat. Res., Rev. Genet. Toxicol.* **1996**, *365*, 129−146.
(16) Kim, H.-S.; Ahn, D.-S.; Chung, S.-Y.; Kim, S. K.; Lee, S. Tautomerization of Adenine Facilitated by Water: Computational Study of Microsolvation. *J. Phys. Chem. A* **2007**, *111*, 8007−8012.
(17) Geerlings, P.; De Proft, F.; Langenaeker, W. Conceptual Density Functional Theory. *Chem. Rev.* **2003**, *103*, 1793−1874.
(18) Bader, R. F. W. *Atoms in Molecules - A Quantum Theory*; The International Series of Monographs on Chemistry *22*; Clarendon Press: New York, 1994.
(19) Bader, R. F. W.; Nguyen-Dang, T. T.; Tal, Y. A Topological Theory of Molecular Structure. *Rep. Prog. Phys.* **1981**, *44*, 893−948.
(20) Krokidis, X.; Noury, S.; Silvi, B. Characterization of Elementary Chemical Processes by Catastrophe Theory. *J. Phys. Chem. A* **1997**, *101*, 7277−7282.
(21) Becke, A. D.; Edgecombe, K. E. A Simple Measure of Electron Localization in Atomic and Molecular Systems. *J. Chem. Phys.* **1990**, *92*, 5397−5403.
(22) Silvi, B.; Savin, A. Classification of Chemical Bonds Based on Topological Analysis of Electron Localization Functions. *Nature* **1994**, *371*, 683−686.
(23) Thom, R. *Structural Stability and Morphogenesis, an Outline of a General Theory of Models*; Benjamin/Cummings Publishing Co.: Reading, MA, 1980.
(24) Adjieufack, A. I.; Mbouombouo Ndassa, I.; Patouossa, I.; Ketcha Mbadcam, J.; Safont, V. S.; Oliva, M.; Andrés, J. On the Outside Looking in: Rethinking the Molecular Mechanism of 1,3-Dipolar Cycloadditions from the Perspective of Bonding Evolution Theory. The Reaction between Cyclic Nitrones and Ethyl Acrylate. *Phys. Chem. Chem. Phys.* **2017**, *19*, 18288−18302.
(25) Adjieufack, A. I.; Liégeois, V.; Mbouombouo Ndassa, I.; Ketcha Mbadcam, J.; Champagne, B. Intramolecular [3 + 2] Cycloaddition Reactions of Unsaturated Nitrile Oxides. A Study from the Perspective of Bond Evolution Theory (BET). *J. Phys. Chem. A* **2018**, *122*, 7472−7481.
(26) Frisch, M.; Trucks, G. W.; Schlegel, H. B.; Scuseria, G. E.; Robb, M. A.; Cheeseman, J. R.; Scalmani, G.; Barone, V.; Mennucci, B.; Petersson, G. A.; et al. *Gaussian 09*, Revision D. 01; Gaussian Inc.: Wallingford, CT, 2014.
(27) Chai, J.-D.; Head-Gordon, M. Long-Range Corrected Hybrid Density Functionals with Damped Atom-Atom Dispersion Corrections. *Phys. Chem. Chem. Phys.* **2008**, *10*, 6615−6620.
(28) Fukui, K. Formulation of the Reaction Coordinate. *J. Phys. Chem.* **1970**, *74*, 4161−4163.
(29) Gonzalez, C.; Schlegel, H. B. Reaction Path Following in Mass-Weighted Internal Coordinates. *J. Phys. Chem.* **1990**, *94*, 5523−5527.
(30) Gonzalez, C.; Schlegel, H. B. Improved Algorithms for Reaction Path following: Higher-Order Implicit Algorithms. *J. Chem. Phys.* **1991**, *95*, 5853−5860.
(31) Tomasi, J.; Mennucci, B.; Cammi, R. Quantum Mechanical Continuum Solvation Models. *Chem. Rev.* **2005**, *105*, 2999−3094.
(32) Noury, S.; Krokidis, X.; Fuster, F.; Silvi, B. Computational Tools for the Electron Localization Function Topological Analysis. *Comput. Chem.* **1999**, *23*, 597−604.
(33) Liégeois, V. *DrawMol*; UNamur, www.unamur.be/drawmol, 2018.
(34) Liégeois, V. *DrawProfile*; UNamur, www.unamur.be/drawprofile, 2018.
(35) Cherni, E.; Essalah, K.; Besbes, N.; Abderrabba, M.; Ayadi, S. Theoretical Investigation of the Regioselective Ring Opening of 2-methylaziridine. Lewis Acid Effect. *J. Mol. Model.* **2018**, *24*, 309.
(36) Catak, S.; D'hooghe, M.; Verstraelen, T.; Hemelsoet, K.; van Nieuwenhove, A.; Ha, H.-J.; Waroquier, M.; Kimpe, N. de; van

https://dx.doi.org/10.1021/acs.jpca.0c01792
J. Phys. Chem. A 2020, 124, 4068−4080

Speybroeck, V. Opposite Regiospecific Ring Opening of 2-(cyanomethyl) Aziridines by Hydrogen Bromide and Benzyl Bromide: Experimental Study and Theoretical Rationalization. *J. Org. Chem.* **2010**, *75*, 4530−4541.
(37) Dahl, O. Interaction of Heat and Drugs in Vitro and in Vivo. In *Thermoradiotherapy and Thermochemotherapy*; Springer: Berlin, 1995; pp 103−121.
(38) Johnson, H. A.; Pavelec, M. Thermal Enhancement of Thio-TEPA Cytotoxicity. *Temp. Chem. Toxicity* **1973**, *50*, 903−908.
(39) Rinne, M. L.; He, Y.; Pachkowski, B. F.; Nakamura, J.; Kelley, M. R. N-methylpurine DNA Glycosylase Overexpression Increases Alkylation Sensitivity by Rapidly Removing Non-Toxic 7-Methylguanine Adducts. *Nucleic Acids Res.* **2005**, *33*, 2859−2867.

https://dx.doi.org/10.1021/acs.jpca.0c01792
J. Phys. Chem. A 2020, 124, 4068−4080